JOURNAL OF CATALYSIS **164,** 322–333 (1996)
ARTICLE NO. 0388

The Influence of Alkali Metal Ions in the Chemisorption of CO and CO_2 on Supported Palladium Catalysts: A Fourier Transform Infrared Spectroscopic Study

Leonarda F. Liotta,* Guy A. Martin,† and Giulio Deganello*,‡

*Istituto di Chimica e Tecnologia dei Prodotti Naturali del CNR (ICTPN-CNR), Via Archirafi 26-28, 90123 Palermo, Italy; †Institut de Recherches sur la Catalyse, CNRS, 2 Avenue Albert Einstein, 69626, Villeurbanne Cédex, France; and ‡Dipartimento di Chimica Inorganica, Università di Palermo, Via Archirafi 26-28, 90123 Palermo, Italy

Received October 6, 1995; revised June 3, 1996; accepted August 9, 1996

Two series of palladium-based catalysts were compared on the basis of the adsorption of CO and CO_2, monitored by Fourier transform infrared spectroscopy. The first series is represented by a silica-supported palladium catalyst and by some catalysts derived from it by addition of different amounts of sodium ion, $0 \leq R \leq 25.6$, where R is the atomic ratio Na/Pd. The second series consists of palladium catalysts supported on "model" and natural pumices. The model pumices, obtained by sol-gel techniques, are silico-aluminates containing variable amounts of sodium so that the corresponding Pd catalysts have an R value in the range $0 \leq R \leq 6.1$. In the Pd/natural pumice catalysts, changes of the atomic ratio $R' = (Na + K)/Pd$ are achieved with different palladium loadings. Despite the analogous behaviour of the catalysts of both series when $R = 0$, the presence of increasing alkali metal ions induces different behaviour towards the adsorption of CO. On increasing R in the Na–Pd/SiO_2 series there is a progressive weakening of the C–O bond to produce eventually carbonates, whereas only a decrease of the amount of adsorbed CO occurs in the Pd/model pumice series ($R \leq 6.1$). Furthermore, only physisorbed CO bands are observed in Pd/natural pumice catalysts ($R' \leq 17$). Different behaviour is also noticed towards the adsorption of CO_2: the equilibrium $CO_2(gas) \rightleftharpoons CO_{ads} + O_{ads}$ occurs in the Pd/SiO_2 series, in contrast to the Pd/pumice series where only carbonate species on the surface of the support are detected. The results are interpreted on the basis of geometric and electronic effects attributed to the different localization of the alkali metal ions in the catalysts. Decoration of palladium by the alkali metal ions is evident on increasing R in the Pd/silica series; such a decoration does not occur in Pd/pumice catalysts at any R or R' value. Accordingly, the behaviours of both series of catalysts towards the chemisorption of CO and CO_2 are interpreted assuming that geometric effects are predominant in the Pd/silica series, whereas in the Pd/pumice series electronic effects are the most important, geometric effects being practically absent.

INTRODUCTION

Alkali ions have long been known (1, 2) to improve the lifetime as well as to modify the activity and selectivity of metal catalysts. Examples (3, 4) of change of activity and selectivity by addition of alkali ions have been reported for Ni/SiO_2 (5, 6), Pd/SiO_2 (7–13), and Pd/Al_2O_3 (14) in several catalyzed reactions.

The presence of alkali ions in supported palladium catalysts is always associated with a negative shift of the Pd-3*d* binding energies as observed by XPS (15–17). In a recent XPS study on Pd/pumice catalysts (18), the electronic charges on the palladium atoms were estimated through the combination of the photoelectron and the Auger shifts yielding the Auger parameter: the latter was found to increase with decrease of the metal crystallite size. These results provided some insight into the interpretation of the peculiar behaviour of pumice-supported palladium catalysts (19). Indeed, the presence of alkali ions in the structure of the natural support increases the range of application of these catalysts towards higher metal dispersions in the selective hydrogenation of highly unsaturated hydrocarbons (20–23); the enhancement of electron density on the metal induces a slow decay of turnover frequency (TOF) vs metal dispersion (D_x) by progressively reducing the strength of interaction of the metal with the electron-rich hydrocarbons. On the contrary, the drastic decrease of TOF in the hydrogenation of alkadienes and alkynes which is usually found (24, 25) with Pd catalysts on traditional supports (silica, alumina, carbon, etc.) when D_x becomes higher than 20%, was attributed to a loss of metallic character in the small metal crystallites which interact too strongly with the electron-rich hydrocarbons (26, 27). This explanation is supported by XPS measurements showing a positive shift of the Pd-3*d* binding energies of small Pd particles (28, 29) in these catalysts.

The distribution of potassium on silica-supported nickel and palladium catalysts, as determined by a high-spatial-resolution scanning transmission electron microscope equipped with an EDX (energy dispersive X-ray) spectrometer (30), was uniform on both the support and the metal particles with higher concentration on nickel than on palladium. LEIS and TEM studies (31) confirm that the

0021-9517/96 $18.00

alkali additive decorates the metal particles of the Pd/silica catalysts doped with sodium ions, but no decoration of palladium by alkali ions was detected in Pd/pumice catalysts. Despite these structural differences both Pd/pumices and alkali-promoted Pd/silica catalysts show the characteristic negative shifts of the Pd-3*d* binding energies in XPS measurements (15–17).

The use of CO as a probe to establish electronic as well as structural characteristics of supported metal catalysts (32) is a well-documented technique, but no comparative studies have so far appeared on the possible differences produced by alkali metal ions when they are present in the structure of the support, as in natural and model (33) pumices, or added as dopants to the Pd/silica catalysts.

In this article we report an FTIR spectroscopic study of the chemisorption of CO and CO_2 on Pd/natural pumice, Pd/model pumices and sodium-promoted Pd/silica samples and show the different role of alkali metal ions in these respective catalysts.

EXPERIMENTAL

All experimental procedures were performed in standard Schlenk glassware under an atmosphere of prepurified nitrogen. Anhydrous alcohols (Aldrich) were prepared according to literature procedures (34) and distilled under nitrogen just before use.

All other chemicals were of reagent grade purity and were used without further purification.

Preparation of Supports and Catalysts

The preparation of the synthetic supports was based on sol-gel techniques according to published procedures (35–37), slightly modified (33) to obtain the desired percentage of the component oxides, SiO_2, Al_2O_3, Na_2O.

In a typical preparation, a solution of $Al(O\text{-}sBu)_3$ in anhydrous sec-butanol (100 ml) and of MeONa in anhydrous methanol (10 ml) were added to a stirred solution of $Si(OEt)_4$ in anhydrous ethanol (100 ml). Relative amounts of the three alkoxides were used accordingly to give the desired composition $SiO_2/Al_2O_3/Na_2O$ (see Table 1). The hydrolysis was performed immediately by adding H_2O in a fivefold excess of the required stoichiometric amount and refluxing the reaction mixture for 3 h. After cooling at room temperature a gel was obtained which was filtered and washed with the anhydrous alcohols. The product was calcined in air ($Synt_1$ at 1023 K, $Snyt_2$ at 1073 K, $Synt_3$ at 1273 K) and crushed. The fractions of 60–70 mesh were used to prepare the catalysts. The characteristics of the supports are listed in Table 1.

The preparation of the supported palladium catalysts on silica and on model pumices was performed using $[Pd(NH_3)_4](NO_3)_2$ according to literature methods (38–40). Silica (Aerosil Degussa, 200 m^2/g) was added to a solution of $[Pd(NH_3)_4](OH)_2$, obtained by ionic exchange from $[Pd(NH_3)_4](NO_3)_2$, in aqueous solution contacted with a resin (Amberlite IRA 400 regenerated in KOH, 0.5M) and stirred for 2 h. The suspension was centrifuged and washed with H_2O (five times); the residual water was evaporated under reduced pressure and the solid was calcined in oxygen at 573 K (0.2 K/min) thus obtaining a Pd^{n+}/SiO_2 support with 1.5% Pd (w/w) content. Fractions of this precursor were added to a solution of $NaNO_3$ and stirred for 2 h. The mixture was evaporated to dryness in a rotary evaporator under reduced pressure and reduced for one night in a flux of H_2 (4 l/h) after increasing the temperature linearly at 2 K/min up to 573 K. The same procedure, without addition of the $NaNO_3$ solution, was used to prepare the Pd/model-pumice catalysts denoted $synt_x$ ($x = 1-3$). The co-precipitation of alcoholates allows incorporation of sodium ions in the framework of model pumices and the ionic exchange of Pd^{2+} and H^+ ions at pH 8.5 avoids any exchange of Na^+ and Pd^{2+}.

TABLE 1

Type, Chemical Composition, and Morphology of the Supports

Type	SiO_2 (%)	Al_2O_3 (%)	Na_2O (%)	K_2O (%)	H_2O (%)	B.E.T (m^2/g)	Morphology (WAXS)
SiO_2	100	—	—	—	—	200	crystalline
$synt_1$	84.27	14.39	—	—	1.34	81	amorphous
$synt_2$	83.55	14.35	0.6	—	1.50	43	amorphous
$synt_3$	83.37	14.24	1.44	—	0.95	12	amorphous[a]
pumice[b]	85.5	6.8	2.0	3.2	2.5	7	amorphous

[a] Some crystallinity is present.
[b] Surface composition (by XPS), after HNO_3 treatment.

The content in alkali metal and the atomic ratio $Na/Pd = R$ are listed in Table 2, together with the metal dispersion (41, 42) and other structural and surface characterization data for both the silica-supported and the model (33) pumice-supported palladium catalysts. The Pd/natural pumice samples used in this work were described previously (43) and their characteristics are also listed in Table 2.

Structural Investigations

BET analyses were carried out on a Carlo Erba Sorptomatic Instrument. Wide angle X-ray scattering (WAXS) analysis of the supports was performed on a Philips vertical goniometer connected to a highly stabilized generator (Siemens Kristalloflex 805). Ni–Cu/Kα filtered radiation was employed and the diffracted beam was monochromatized with a focusing graphite monochromator (Bragg–Brentano geometry). A proportional counter and 0.05° step sizes in 2θ were used with an accumulated counting time of 100 s per angular abscissa.

The metal particle sizes of Pd/silica catalysts were determined by Transmission electron microscopy (TEM)

TABLE 2

Structural and Surface Characteristics of Supported Pd Catalysts

Catalyst[a]	*R* ratio	*R′* ratio	Pd (% wt)	Na (% wt)	*K* (% wt)	D_H (%)[b]	TEM (nm)[c]	SAXS (nm)	$Shift_{XPS}$
Pd/SiO_2	0.0	—	1.50	0.00	0.0	70	1.7[d]	—	n.d.
$Na–Pd/SiO_2$	0.4	—	1.50	0.13	0.0	62	3.0	—	n.d.
$Na–Pd/SiO_2$	1.6	—	1.50	0.52	0.0	56	n.d.	—	n.d.
$Na–Pd/SiO_2$	6.4	—	1.50	2.08	0.0	52	2.0–6.0	—	n.d.
$Na–Pd/SiO_2$	25.6	—	1.50	8.32	0.0	49	n.d.	—	−0.80[e]
$Pd/synt_1$	0.0	—	1.20	0.00	0.0	65	n.d.	—	−0.10[e]
$Pd/synt_2$	2.1	—	0.95	0.44	0.0	50	2.0–6.0	—	−0.51[e]
$Pd/synt_3$	6.1	—	0.80	1.06	0.0	47	4.0–10.0	—	−1.0[e]
Pd/pumice	—	17.0	0.86	1.49	2.78	28	n.d.	5.3[f]	−0.5
Pd/pumice	—	12.8	1.14	1.48	2.77	22	n.d.	6.1[f]	n.d.

[a] All the catalysts were analyzed before and after the reduction with H_2 and no difference was found.
[b] Determined by the methods of Aben (41) and Benson *et al.* (42); the results are quite similar with both methods.
[c] See Ref. (31).
[d] This work, average size diameter.
[e] See Ref (78).
[f] See Ref. (43).

Analysis in a JEOL 100X electron microscope. To avoid dissolution of alkali metal ions in the liquid phase, the reduced samples were prepared by sedimentation of an aerosol of powdered catalyst on a carbon-coated copper grid. The average diameters of the palladium particles are listed in Table 2.

Fourier Transform Infrared (FTIR) Studies

FTIR analyses were performed on catalyst discs (diameter 18 mm, weight 20–30 mg), placed on a quartz holder, and introduced into a cell which allowed *in situ* reduction. The adsorbed hydrogen was eliminated by pumping at 573 K for 1 h. After cooling the cell at 298 K, carbon monoxide (or carbon dioxide) was introduced at 1 Torr pressure. The cell was then evacuated at increasing temperature (0.5 h at 298 K and 323 K, 1 h at higher temperatures). The Pd/silica samples were analyzed with an IES 110 Bruker spectrophotometer with a resolution of 4 cm^{-1}, while the Pd/pumice samples, owing to the poor transparency of the supports, were analyzed with a Nicolet 550 spectrophotometer working in diffuse reflectance with a resolution of 0.125 cm^{-1}.

Each spectrum shown in this article resulted from the difference between the spectrum of the sample with the gas (CO or CO_2) at the various temperatures and the spectrum at the same temperature of the pure catalyst reduced in hydrogen and degassed. Subtracted spectra were obtained, at a scaling factor 1, to eliminate all the Si–O overtones in the range 2100–1600 cm^{-1}. Each vibrational spectrum was smoothed and the same operations were performed on the two original spectra to be sure that no band was subtracted or added by the mathematical artefacts used.

Several functions were tested for the deconvolution of the spectra: Gaussian, Lorentzian, a function product Gaussian–Lorentzian, and a function sum Gaussian–Lorentzian. For the simplest spectra, analysis of the residue absorbance was also performed. Deconvolution of the spectra shown in the figures is that resulting from a multiple Lorentzian function, performed with Peakfit software, using a basic program. The fitting with this multiple Lorentzian function gave the best standard deviation.

The sum of the elementary bands reproduces quite well the experimental spectra. For each band the following parameters were obtained: the position of the maximum δ in cm^{-1}, the intensity, and the full width at half maximum of the peak.

RESULTS AND DISCUSSION

Silica-Supported Palladium Catalysts

The FTIR spectrum of the CO chemisorbed on the Pd/SiO_2 catalyst, after evacuation of the gas at 298 K, is reported in Fig. 1.

Deconvolution of the spectrum gives five elementary bands (Fig. 1) at 2095, 2080, 1983, 1963, and 1923 cm^{-1}. These bands are similar to those reported by several authors on supported (44–52) and unsupported Pd (53–55). The band at 2095 cm^{-1} could be attributed to a linear CO chemisorbed on low coordination sites (corner or edge surface sites (56) of faces of high crystallographic index), similar to that found in a FTIR study of a series of Ni/SiO_2 catalysts (57). The other bands can be assigned to linear CO ($\nu CO = 2080$ cm^{-1}) (44, 50, 58), bridging CO ($\nu CO =$ 1983 cm^{-1}), adsorbed on the [100] face (44, 50, 52, 58) and to multibonded CO species ($\nu CO = 1963$, 1923 cm^{-1}) adsorbed on the [111] face of Pd crystallites (53–55), respectively. According to the literature (51) carbon monoxide

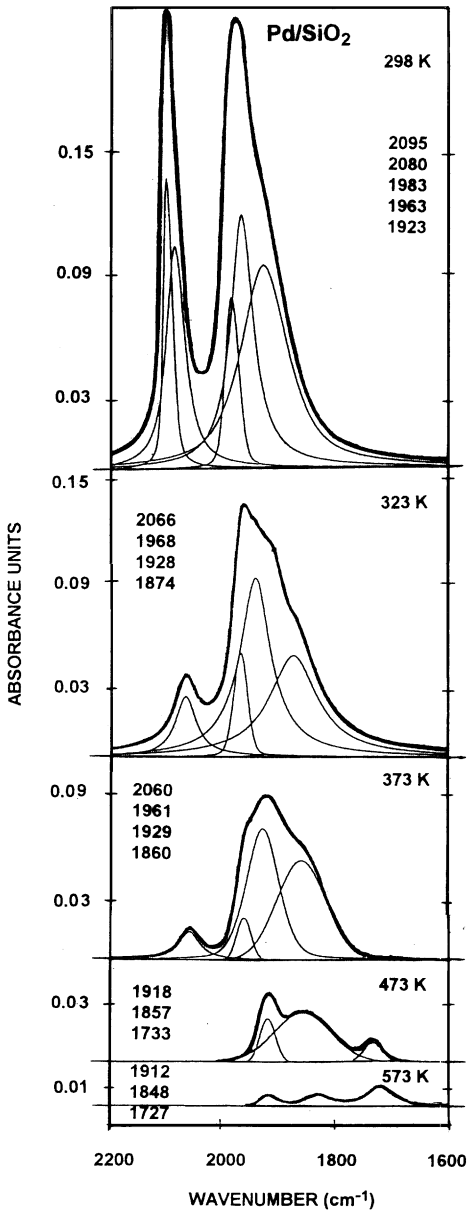

FIG. 1. Infrared spectra of irreversibly adsorbed CO over Pd/SiO_2 catalyst ($R = 0$) after pumping at 298 K (0.5 h), 323 K (0.5 h), 373 K (1 h), 473 K (1 h), and 573 K (1 h). The columns of numbers reported in each spectrum are the wavenumber (cm^{-1}) values of the deconvoluted bands indicated.

adsorbs on Pd surface as bridging CO, but if the pressure of CO is increased some linear species are obtained; only after pumping at temperatures higher than 298 K do the linear species convert into the bridging ones. Moreover, at high CO coverage all the bands of the IR spectrum are shifted towards higher frequencies because of an increased "through space" dipolar interaction (CO–CO) (54). This occurrence was confirmed by the small upfield shifts in the CO frequencies of spectra registered at higher CO pressures (10 and 20 Torr).

After pumping at 323 K the band at 2095 cm^{-1} disappears. At increasing temperature, the linear CO ($\nu CO = 2080\ cm^{-1}$) decreases in intensity and disappears at 473 K (Fig. 1); the bands due to bridging and multibonded CO disappear at 623 and 673 K, respectively. Due to the decrease of dipolar interaction, the wavenumbers of these bands are shifted downwards and the νCO values, at vanishing coverage, are found to be 2060, 1961, 1912, and 1848 cm^{-1}, respectively.

The addition of Na^+ to the Pd/silica catalyst produces a slight decrease of metal dispersion (Table 1) and perturbs the IR spectra. The effects of this perturbation are quite clearly related to R (atomic ratio Na/Pd) (Table 2) since all the changes in the bands associated with the adsorption of CO in the starting Pd/SiO_2 catalyst become more marked as the above ratio increases. The irreversible chemisorption of CO at 298 K over the catalyst with $R = 0.4$ results in a shift of the bands attributed to linear CO and bridging CO towards lower frequencies ($\Delta\nu_1 = 12\ cm^{-1}$ and $\Delta\nu_2 = 17\ cm^{-1}$, respectively) and in a significant intensity decrease; a new band develops at 1885 cm^{-1} (Figs. 2 and 3). These effects are more pronounced on increasing the R values in the series: at $R = 1.6$, $\Delta\nu_1 = 24\ cm^{-1}$, $\Delta\nu_2 = 38\ cm^{-1}$, $\Delta\nu_3 = 67\ cm^{-1}$; at $R = 6.4$ the linear CO band disappears, $\Delta\nu_2 = 46\ cm^{-1}$, $\Delta\nu_3 = 82\ cm^{-1}$; at $R = 25.6$ all the carbonyl bands disappear. These shifts cannot be solely accounted for by a possible decrease of the dipole–dipole interaction induced by the presence of sodium ions; as an example the wavenumber corresponding to the bridged species on $Na–Pd/SiO_2$ ($R = 1.6$) (Figs. 2 and 4), after outgassing at 298 K (1945 cm^{-1}) is lower by $\Delta\nu_2 = 16\ cm^{-1}$ than that observed on unpromoted Pd/SiO_2 at low coverage (1961 cm^{-1}) (Fig. 1). Shifts at higher R value are still larger (Fig. 5). Furthermore, sodium addition to Pd/SiO_2 results in an intensity decrease of the linear and bridged species with increasing R (Table 3) which cannot be solely accounted for by the increase of Pd particle size (Table 2). These results can be explained by the occurrence of three effects arising from the increased Na/Pd atomic ratio, as detailed below:

(i) The increase of sodium coverage of the palladium surface as R increases produces a decorating effect already

TABLE 3

Effect of Alkali Metal Ion Addition on the Bridging CO/linear CO Ratio in Pd/SiO_2 Catalysts

Catalyst	R ratio	Intensity CO band		B/L ratio
		Bridged CO(B)	Linear CO (L)	
Pd/SiO_2	0.0	0.08691	0.09481	0.92
$Na–Pd/SiO_2$	0.4	0.02307	0.00576	4.01
$Na–Pd/SiO_2$	1.6	0.00341	0.00221	1.55
$Na–Pd/SiO_2$	6.4	0.01071	—	—
$Na–Pd/SiO_2$	25.6	—	—	—

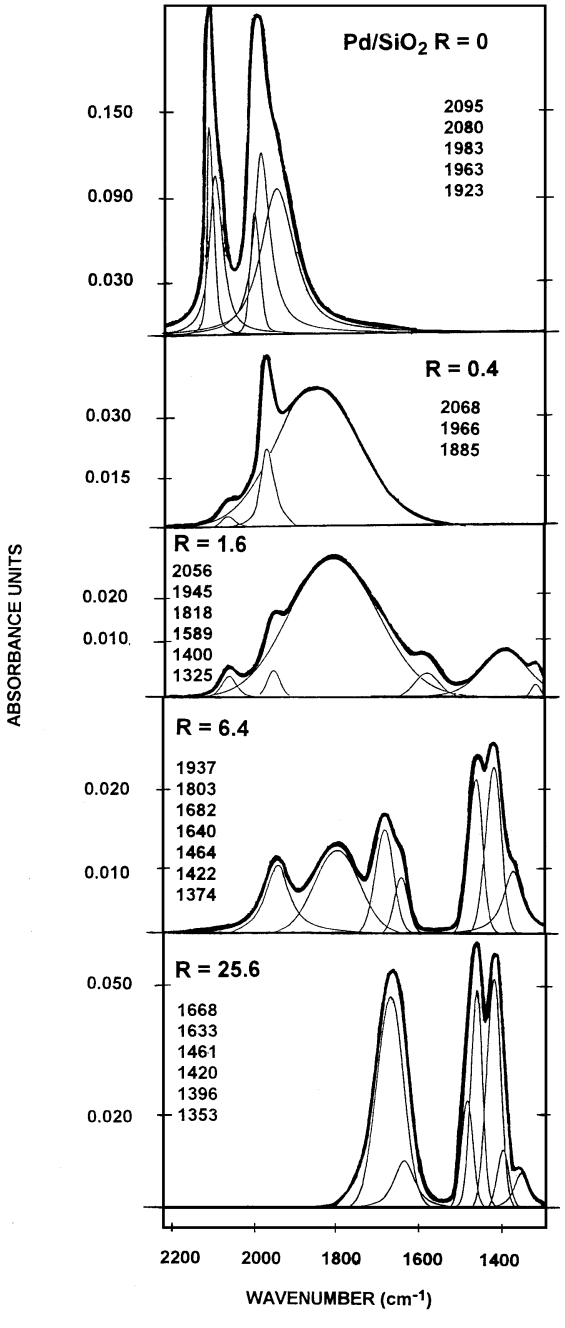

FIG. 2. Infrared spectra of irreversibly adsorbed CO at 298 K over Na–Pd/SiO_2 catalyst at different R = Na/Pd atomic ratios.

known for alkali-promoted Ni/SiO_2 catalysts (59). This effect inhibits the adsorption of CO on the metal and is documented by the decrease in the intensity of the bands at higher frequencies (linear CO and bridging CO).

(ii) According to the well-documented effect in coordination chemistry of a downwards shift of the carbonyl stretching frequency when a Lewis acid, such as an alkali ion, interacts with the oxygen of the carbonyl ligand in metal carbonyl complexes, resulting in a decrease of C–O bond

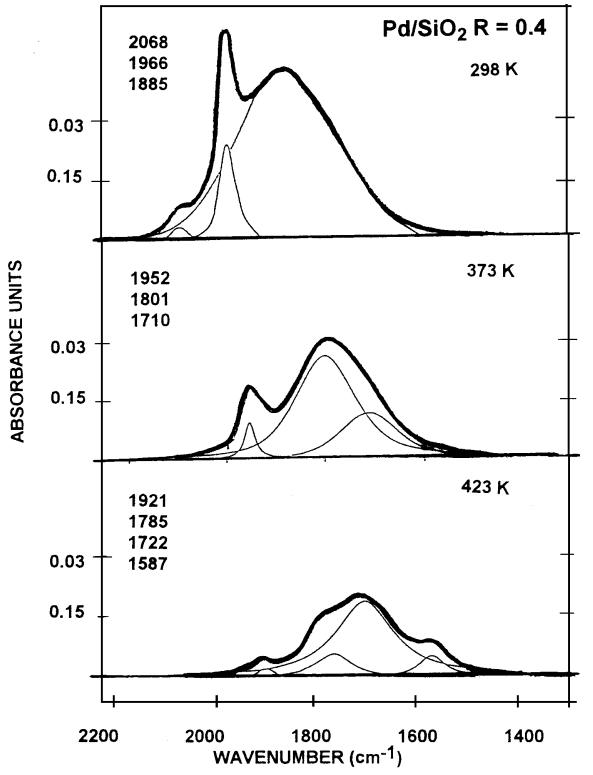

FIG. 3. Infrared spectra of irreversibly adsorbed CO over Na–Pd/SiO_2 ($R = 0.4$) after pumping at increasing temperatures.

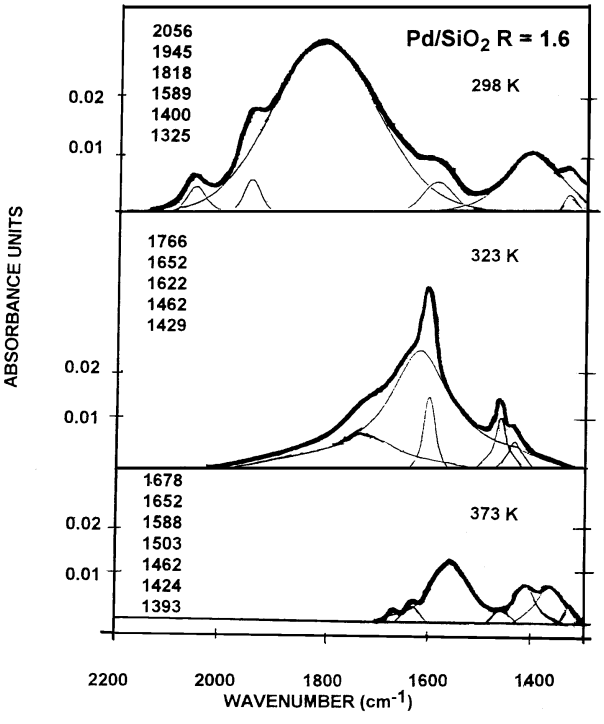

FIG. 4. Infrared spectra of irreversibly adsorbed CO over Na–Pd/SiO_2 ($R = 1.6$) after pumping at increasing temperatures.

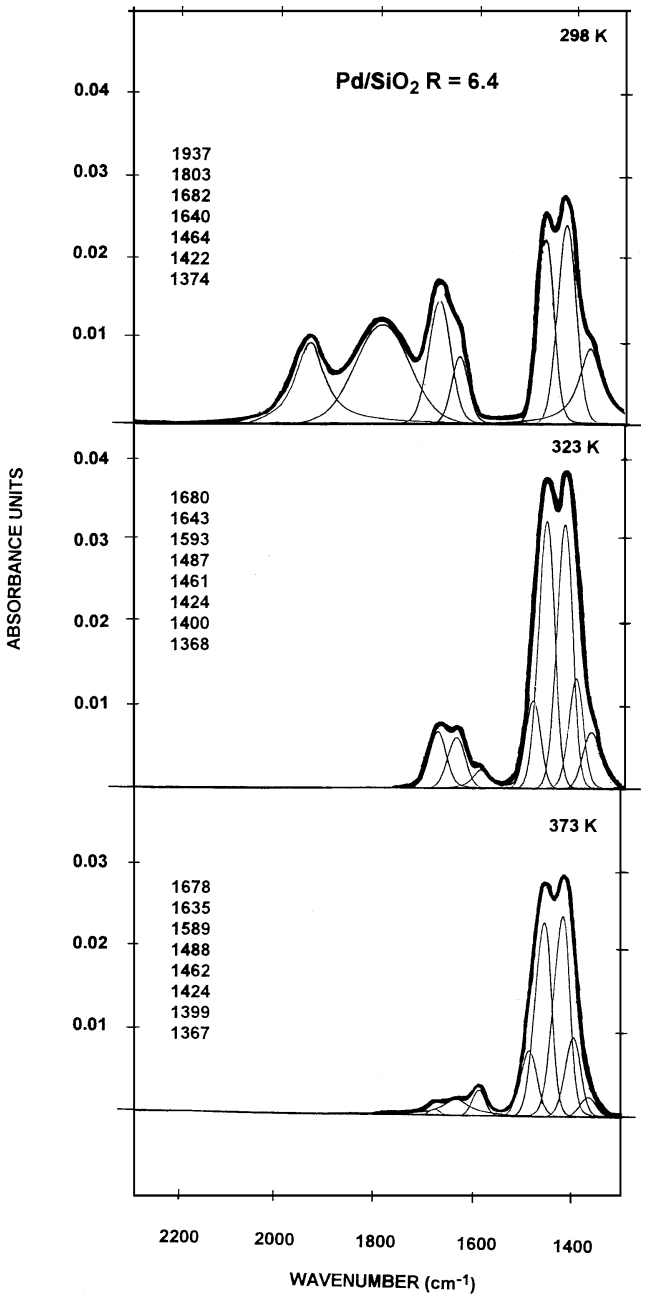

FIG. 5. Infrared spectra of irreversibly adsorbed CO over Na–Pd/SiO_2 ($R = 6.4$) after pumping at increasing temperatures.

order (60), the presence of the new band at lower frequency (61–64) (see Table 4), already found in alkali promoted Ni/SiO_2 (65–67) and Pd/SiO_2 (33, 68, 69) catalysts, has been attributed to a $Pd–CO–Na^+$ species. When the sodium promoter is added to the Pd/SiO_2 catalyst it can be seen that the bridging/linear ratio increases from 0.92 to 4.01 when $R = 0.4$. The decrease of metal dispersion resulting from sodium addition can account for a part of this increase: as a matter of fact, it was shown (52) that when the dispersion of palladium decreases from 70 to 62% (Pd/SiO_2 and $Na–Pd/SiO_2$, respectively) this ratio goes from 2.5 to 3. Thus, sodium addition produces per se an increase of the bridging/linear ratio which can be explained by an evolution of the linear species into the $Pd–CO–Na^+$ band.

(iii) The negative shift of the Pd-3*d* binding energies observed by XPS (15) in Pd/SiO_2 catalysts doped with alkali metal ions is indicative of an increased electron density on the metal due to the presence of alkali ions. This increase of palladium electron density gives rise to the increasing shift towards lower frequencies of all the carbonyl bands of the Pd/SiO_2 catalysts as *R* increases, through a decreased bond order of the C–O linkage resulting from the increased back-donation of electron density from Pd-3*d* orbitals on the antibonding π molecular orbitals of coordinated carbonyls. Our preparation conditions and XPS data (15) strongly support the presence of sodium ions also at high *R* ratio and makes unlikely an interaction $Na^+–CO^-$ as in the case of Pd + K/CO system (70).

In principle the decrease of intensity of the carbonyl bands in these IR spectra could be due also to electronic effects; indeed the electron density increase of palladium by the metal alkali ions on the support should decrease the electron donation from the CO highest occupied molecular orbitals (HOMO) to the metal. This contribution, which is essential in the cases of Pd/pumices (see below), could be present in the Na-promoted Pd/SiO_2 catalysts only at low *R* values, since the contribution from geometric hindrance becomes predominant on increasing the *R* values (31).

The intensity of some further bands in the 1680–1320 cm^{-1} region increases with *R* when the samples are evacuated at increasing temperature (Fig. 6). These bands are related to carbonate species formed because of an equilibrium $CO–CO_2$ already known in polycrystalline nickel (71–73) at high temperatures. The complete disproportionation of adsorbed CO into C and CO_2 has been documented in an IR study of Ni/SiO_2 catalysts (72). The addition of alkali, decreasing the C–O bond order through the interaction $Ni–CO–Na^+$ (74), favours the breaking of the C–O bond on the surface so that the disproportionation occurs

TABLE 4

Effect of Alkali Metal Ion Addition on the Frequency of the $Pd–CO–Na^+$ Band in Pd/SiO_2 Catalysts

Catalyst	*R* ratio	Frequency of the $Pd–CO–Na^+$ band (cm^{-1})	
		At high coverage	At low coverage
Pd/SiO_2	0.0	n.o.	n.o.
$Na–Pd/SiO_2$	0.4	1885	1785
$Na–Pd/SiO_2$	1.6	1818	1766
$Na–Pd/SiO_2$	6.4	1803	n.o.
$Na–Pd/SiO_2$	25.6	n.o.	n.o.

Note. n.o.: not observed.

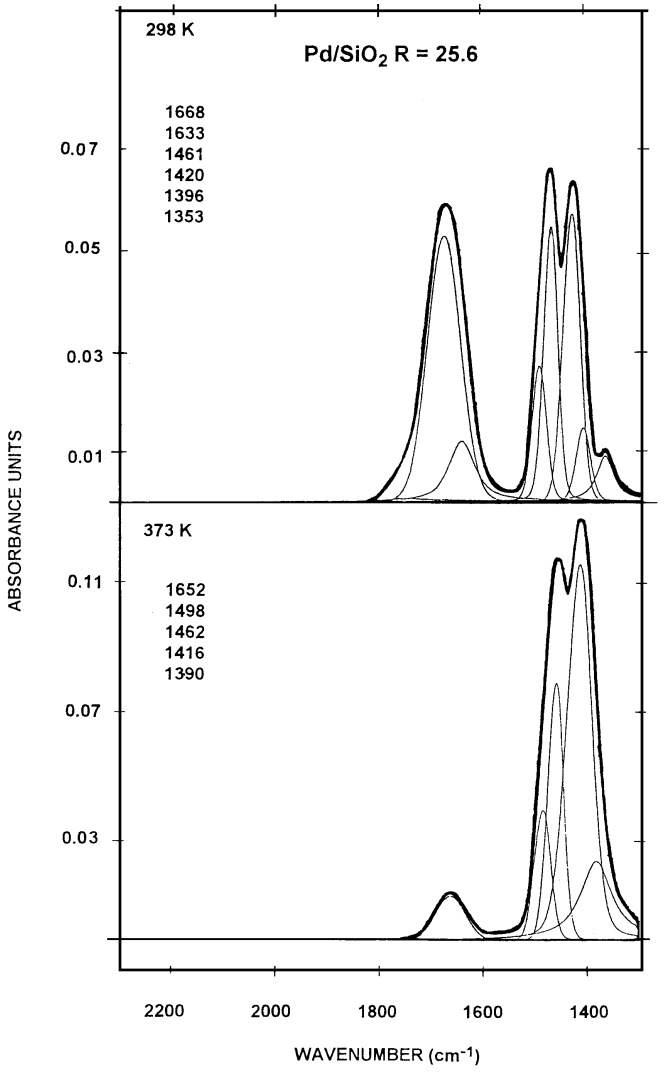

FIG. 6. Infrared spectra of irreversibly adsorbed CO over Na–Pd/SiO_2 ($R = 25.6$) after evacuation at increasing temperatures.

at temperature as low as 300 K (57). Similar behaviour is found in our sodium promoted Pd/SiO_2 catalysts; the intensity of the carbonate bands increases with R and their formation occurs with simultaneous decrease in intensity of the Pd–CO–Na^+ bands, confirming that the origin of carbonate bands results from C–O bond breaking. As pointed out previously, when $R = 25.6$ the IR spectrum does not show any band attributable to Pd–CO–Na^+ but only bands due to carbonate species. Evacuation of the gas phase at higher temperatures ($T > 323$ K) increases the intensity of the carbonate bands (Fig. 6), which disappear at $T \simeq 700$ K. Again the attribution of the bands in the 1680–1320 cm^{-1} region is easily obtained by comparison of the spectra of our Pd/SiO_2 catalysts with those reported for alkali-promoted Ni/SiO_2 catalysts (57). The uni-, bi-dentate, and bridged carbonate forms are detected in the 1570–1370 cm^{-1} region.

To solve the problem of the type and origin of the carbonate thus formed, we studied CO_2 adsorption over Pd/SiO_2 and alkali-promoted Pd/SiO_2 catalysts. The addition of Na^+, besides giving a decrease of the intensity of −OH groups of silica, modifies the basicity of the support and induces adsorption of CO_2 to give alkali carbonates. Another feature is represented by the presence on Pd/SiO_2 of bands in the region of bridging CO (1930 cm^{-1}) and of multibonded CO species (1905 and 1863 cm^{-1}) (Fig. 7). Therefore the adsorption of CO_2 on Pd/SiO_2 catalyst series undergoes the following reversible dissociation:

$$CO_2(\text{gas}) \rightleftharpoons CO_{ads} + O_{ads}$$

already observed in the similar Ni/SiO_2 catalysts (74). CO_2 is adsorbed only in a molecular form on pure SiO_2 giving a band at 2347 cm^{-1} [2340 cm^{-1} in the literature (75)] which disappears after pumping. No evidence of carbonates nor of CO bands was found. On Pd/SiO_2 the above dissociation occurs and, as suggested for the adsorption of CO_2 on Ni/SiO_2 (57), the support could stabilize O_{ads} and form weakly bonded "tail" carbonates (bands at 1640 and 1408 cm^{-1}) (Scheme 1). However, these bands disappear at 298 K after pumping (Fig. 7) and this occurrence is typical of an anionic species CO_2^-, as suggested for the adsorption and reactions of CO_2 on K-modified Rh/SiO_2 (76). The formation of CO_2^- on the support was indicated as prerequisite for the formation of CO_{ads} on the metal (77). The formation of oxygen atoms on the Pd surface, can justify the downward shifts of the bridging and multibonded CO bands in the Pd/SiO_2 catalysts on comparison with the bands of the same nature produced by the direct adsorption of CO: the screening effect of surface O atoms decreases further the CO–CO dipolar interaction (54). The absence of the usual upwards shift of the CO bands originated by

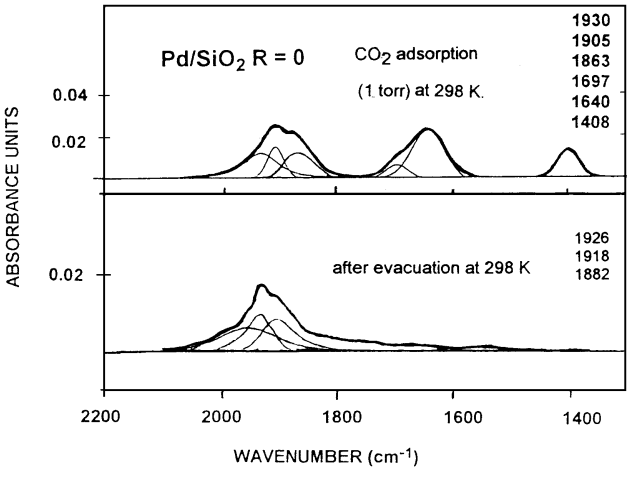

FIG. 7. Formation of Pd–CO bonds by adsorption of CO_2 on Pd/SiO_2 ($R = 0$), at 298 K ($p = 1$ Torr), and after pumping at 298 K for 30 min.

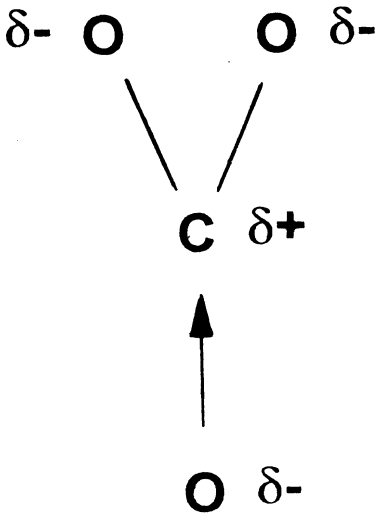

SCHEME 1

CO_2 dissociation is indicative of the incapacity of O_{ads} in oxidizing the supported Pd, so that its influence is limited to a screening of CO bands with a consequent downwards shift of those bands. A similar situation was observed on reaction of CO_2 on Ni/SiO_2 (74). The presence of bridging CO and multibonded CO bands could suggest a mechanism of rupture of the CO_2^- ion which involves two or more adjacent palladium atoms.

Pumice-Supported Palladium Catalysts

As pointed out in the introduction, the negative shifts of the Pd-3*d* binding energies of alkali-promoted Pd/SiO_2 catalysts (15) was also observed for the natural (16–18) and model (33) pumice-supported palladium catalysts (Table 2) (78). The study of these catalysts by LEIS and TEM has shown (31) that the addition of sodium ions to silica-supported catalysts results in a decoration of palladium, in contrast to Pd/natural pumice. To obtain more insight into the properties of these solids we performed the comparative study by FTIR of CO and CO_2 adsorption.

The IR spectrum of CO adsorption on $Pd/synt_1$ ($R = 0$), which differs from Pd/SiO_2 by the substitution of about 14% silica by alumina, is practically the same as that of unpromoted Pd/SiO_2 (Fig. 8). Supported palladium catalysts with high metal dispersion (52), such as our Pd/SiO_2 and $Pd/synt_1$ catalysts, are known to adsorb CO with a larger ratio of the linear over the bridging mode. Since linear CO is adsorbed preferentially on the Pd (110) face (79), one can speculate that in $Pd/synt_1$ the accessibility of the Pd (110) face is higher than in Pd/SiO_2. The shift of a few cm^{-1} in the bands (2093 and 2074 cm^{-1} attributed to linear CO adsorbed on corner and edge (56) or surface (52) sites, respectively, 1970 cm^{-1} to bridging CO (52), 1941 and 1906 cm^{-1} to multibonded CO species (53–55)) could be accounted for by small differences in metal dispersion (51) and/or by the substitution of part of silica by more basic alumina. Again, upon pumping at increasing temperature the usual decrease in intensity and shift of the bands towards lower frequencies (Fig. 9) is observed. Increasing the amount of Na^+ in the model pumices does not change qualitatively the IR spectrum of adsorbed CO: however, the decrease in intensity and in frequency values of the bands (Fig. 10) is more marked than for the case of $Na–Pd/SiO_2$ catalysts. Furthermore, on pumping at 323 K, all the CO bands observed on the $Pd/synt_3$ sample ($R = 6.1$) disappear. The possibility that Pd^{n+} is present on Pd/model pumice catalysts is ruled out since the temperature of reduction of Pd/pumice catalysts (573 K) is sufficient to decompose nitrates, owing to the catalytic effect of Pd (80), and to reduce Pd^{2+} to Pd^0, as shown by XPS, IR, and TPR measurements (33).

While in Pd/SiO_2 the addition of sodium ions modifies the metal surface by decoration of palladium (31), in $Pd/synt_2$

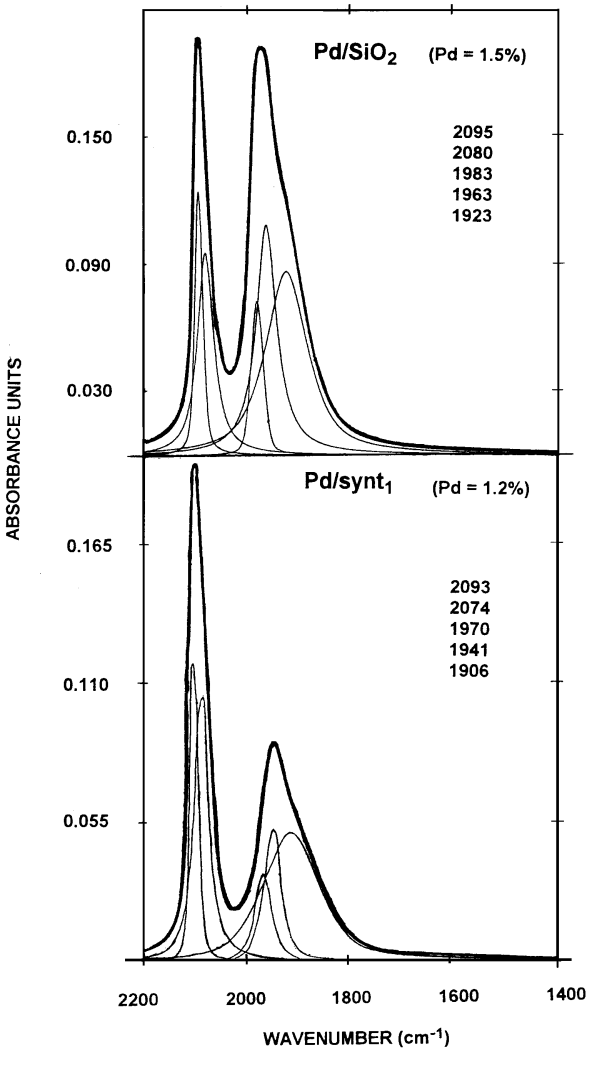

FIG. 8. Comparison of the IR spectra of CO adsorbed on Pd/SiO_2 ($R = 0$) and Pd/model pumice ($R = 0$).

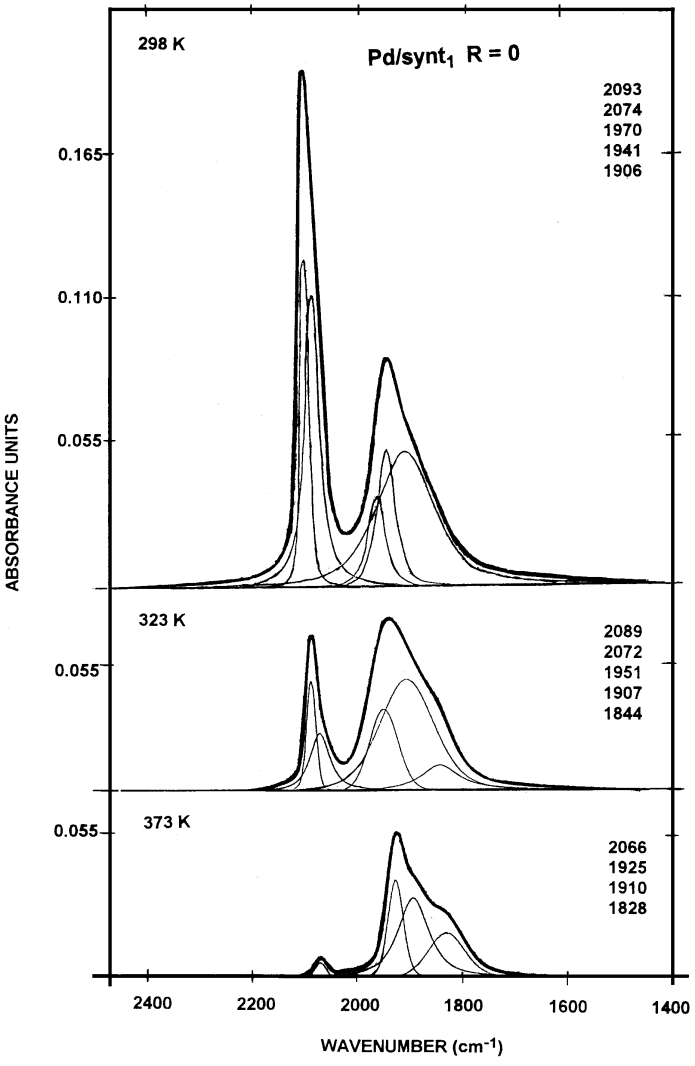

FIG. 9. Adsorption of CO (1 Torr) on Pd/model pumice catalyst ($R = 0$): effect of evacuation at increasing temperature.

and Pd/synt$_3$ the sodium ions are incorporated structurally in the support, which produces exclusively changes in the electronic density of palladium with consequent weakening of the Pd–carbonyl bond. This last effect is still more important in the Pd/natural pumice catalysts for which there is no evidence of CO chemisorption at 298 K. Increasing the CO pressure (20 Torr) and the temperature (373 K) does not result in observable CO chemisorption either. Moreover, no evidence of carbonate formation was found even at 423 K. The low intensity bands (Fig. 11) at 2179 and 2109 cm^{-1}, which are detected under high pressure of CO, disappear after pumping at 298 K and can be assigned to physically adsorbed CO on the surface. Bands in the range 2180–2100 cm^{-1} are attributed to traces of CO gas (52) and we have indeed detected those bands in the IR spectra in CO atmosphere ($p = 1$ Torr) with unpromoted and Na-promoted Pd/SiO_2 samples. These bands, however, disappear on pumping at 298 K. The possibility that the band at 2179 cm^{-1} arises from the chemisorption of CO on a Pd^{n+} site is ruled out by the experimental conditions since all the samples were reduced *in situ* with H_2 before the admission of CO. Furthermore, the difficulty of oxidizing Pd/pumice catalysts is well documented (19, 20). The attribution of the band at 2109 cm^{-1} to an unusually high frequency νCO in linear Pd–CO is very unlikely since the trend of all the Pd–carbonyl bands in the model pumice-supported palladium catalysts shows a shift toward lower frequencies with increasing the Na/Pd atomic ratio; usually the linear bands Pd–CO are found in the 2100–2000 cm^{-1} range (81). In the case of sodium containing Pd catalysts examined in this work, it appears that the decrease in intensity of the linear CO band with increasing Na^+ content is more pronounced in the Na–Pd/SiO_2 series (Fig. 2) than in the Pd/pumice series (Fig. 10a). This result can be easily explained by the transformation in the Na–Pd/SiO_2 catalysts of linear Pd–CO into Pd–CO–Na^+, a procedure impossible in the Pd/pumice series where the Na^+ is in the framework of the support. As shown in Fig. 10c the stability of the linear CO band is limited since at 323 K this band disappears.

As reported in the Experimental section, owing to the poor transparency of the support, the IR spectra of Pd/natural pumice catalysts were recorded in diffuse reflectance on a FT Nicolet 550 spectrophotometer. To confirm that the change of the experimental conditions did not influence the result of the analyses, we performed the record of the adsorption of CO on a Pd/SiO_2 catalyst in the above conditions; the results were identical to those obtained on the IFS 110 Bruker spectrophotometer operating in the transmittance mode. The progressive decrease in intensity and shift in frequency of the bands attributable to chemisorbed CO in Pd/model pumices, when R increases, and the absence of CO chemisorption on Pd/natural pumice catalysts which are characterized by a value of $R' = (Na + K)/Pd$ atomic ratio, higher than R, are interpretable on the basis of simple considerations of the electronic influence of the alkali metal ions in the structure of the pumices. Moreover, the LEIS and TEM experiments (31) on those catalysts show that no decoration of palladium occurs, irrespective of the R' ratio. The electron density on supported palladium was shown to increase with the metal dispersion (18). This effect decreases the σ bond of CO to the metal, thus reducing the intensity of all the CO bands. This occurrence becomes more and more evident as R increases so that in the case of Pd/natural pumice catalysts ($R' = 17$) the adsorption of CO is inhibited. When the Pd–CO bond occurs, however, as in the Pd/synt$_2$ and Pd/synt$_3$ ($R = 2.1$ and 6.1, respectively), the high electron density of palladium produces a shift towards lower values of all the CO frequencies, which can be attributed to a back-donation increase of electron density from palladium orbitals to the CO π^* molecular orbitals (LUMO).

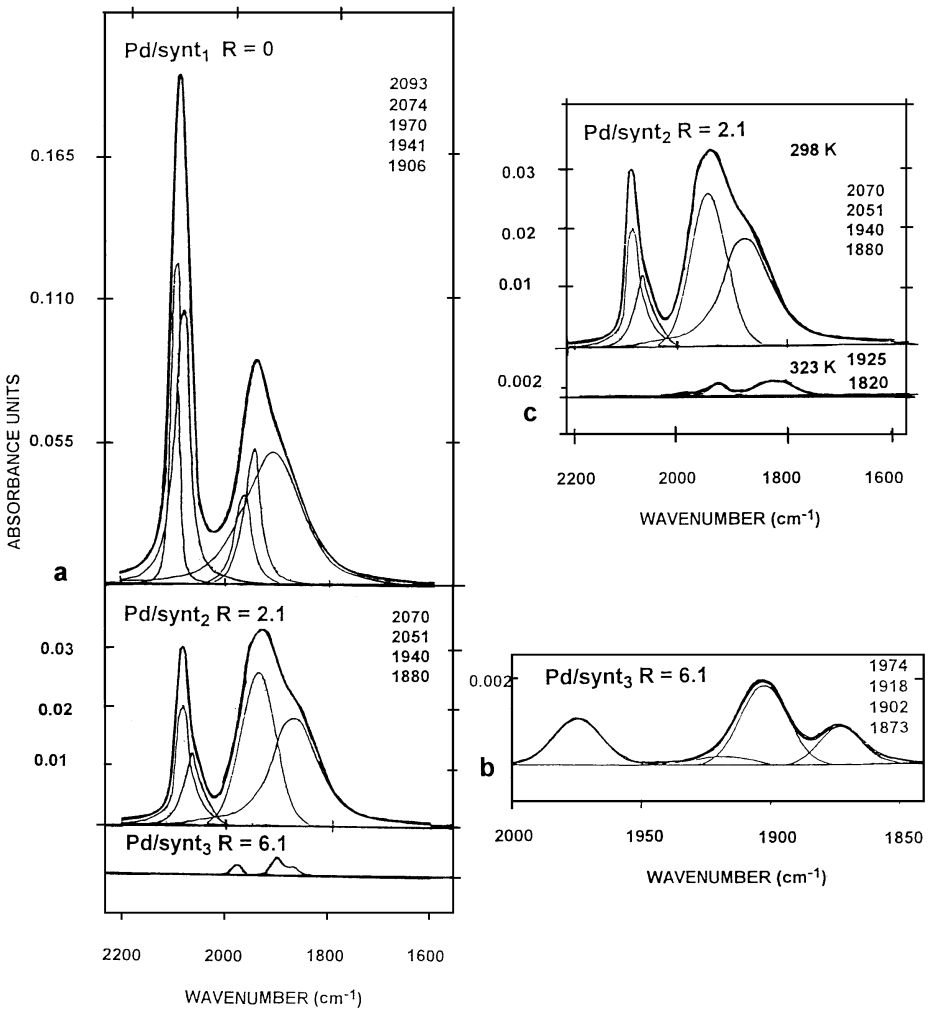

FIG. 10. Adsorption of CO (1 Torr) on Pd/model pumice catalysts on evacuation at 298 K: (a) effect of increasing *R* (b) the enlarged spectrum of $Pd/synt_3$ (c) effect of temperature on $Pd/synt_2$.

This effect, due specifically to the presence of alkali metal ions in the support, should be present also in the series of alkali promoted Pd/SiO_2 catalysts and indeed a shift of the CO band frequencies towards lower value is evident; however, it is likely that the decoration of palladium by Na^+ in those catalysts (31) is the main cause of the decrease of the intensity of the CO bands.

In Pd/pumice catalysts there is no evidence of the equilibrium

$$CO_2(gas) \rightleftharpoons CO_{ads} + O_{ads}$$

already shown for Pd/SiO_2 catalysts. The basic nature of the pumices due to the presence of Al_2O_3 and alkali oxides (Na_2O and K_2O, essentially) is evident from the formation of carbonate bands in the 1640–1386 cm^{-1} region in the IR spectra of the pumice supports under CO_2 atmosphere. No adsorption of CO_2 occurs on Pd since there are no appreciable differences in the IR spectra of Pd/pumice catalysts (Fig. 12). Similar bands were detected in the IR spectra, in CO_2 atmosphere, of samples of alumina and alumina with 2% Na_2O (82).

CONCLUSIONS

This study illustrates the different role of alkali metal ions in supported palladium catalysts depending on whether the alkali promoter is subsequently added to the catalysts or is present as a structural component of the support.

An electronic density transfer to palladium is the common effect of the presence of alkali metal ions in both series of catalysts as already documented by XPS with a shift towards negative values of the Pd 3*d* binding energies (15–18). This effect produces a general shift towards lower frequencies of the CO bands of the IR spectra of chemisorbed CO on these catalysts, owing to an enhanced transfer of electron density from the metal to the π^* molecular orbitals of CO, on increasing *R*.

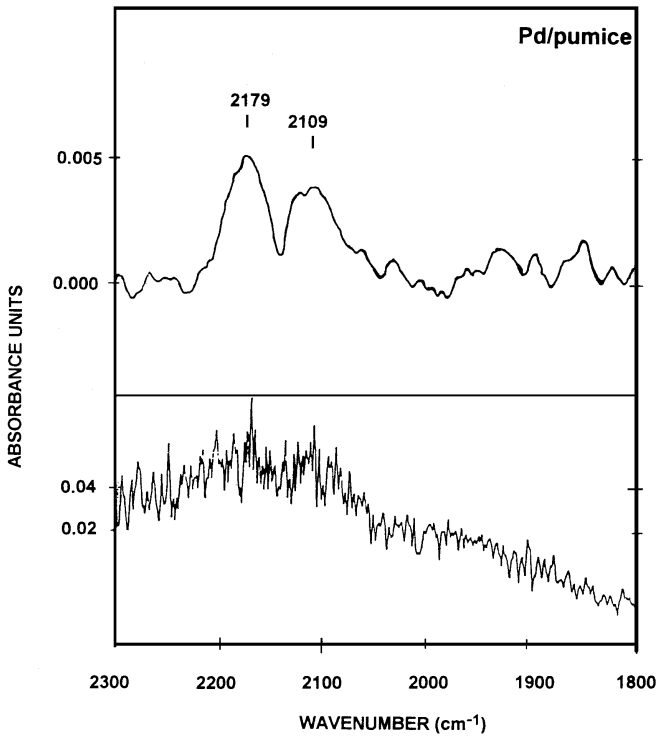

FIG. 11. Physical adsorption of CO on Pd/natural pumice catalyst ($R' = 17$): spectrum under CO (10 Torr) and after evacuation at 298 K.

In addition, an important geometric effect is detected when sodium ions are added to Pd/SiO_2 catalysts. As shown by LEIS and TEM experiments (31), the metal surface is progressively decorated by Na^+ on increasing R, and this occurrence produces eventually dissociation of chemisorbed CO to form carbonate species. On the contrary, even when natural pumice ($(R' = 17)$; $R' = (Na + K)/Pd$ atomic ratio) is the support, the Pd surface is free from alkali ion decoration and the absence of any chemisorption of CO is due again to pure electronic effects. The very high electron density on the metal inhibits the σ bond formation of CO to palladium.

The differences between the two series of catalysts are also illustrated by their behaviour towards CO_2 adsorption: in the case of Pd/SiO_2 catalysts the formation of CO occurs through a dissociation equilibrium

$$CO_2(gas) \rightleftharpoons CO_{ads} + O_{ads}$$

while with Pd/pumice the CO_2 dissociation is not observed: carbonates are only detected on the support surface when CO_2 is adsorbed.

The different role of the alkali metal ions shown in this study can induce dramatic changes in the reactivity of the catalysts. A correct R value in an alkali-promoted Pd/SiO_2 catalyst was found to increase the selectivity towards methanol for the reaction of hydrogenation of carbon monoxide (83). A study of catalytic hydrogenations over Pd/model-pumice catalysts to find the R or R' values for the best activity/selectivity combination is now in progress.

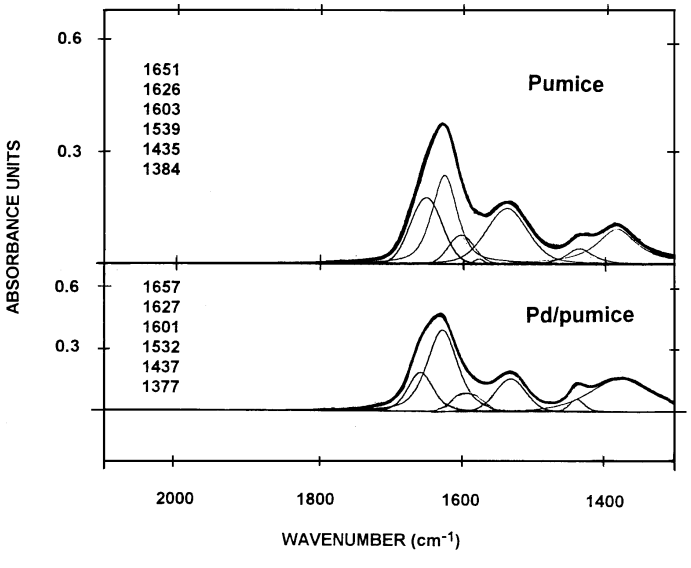

FIG. 12. Infrared spectra obtained after contacting natural pumice and a Pd/natural pumice catalyst with CO_2 at 298 K and evacuation.

ACKNOWLEDGMENTS

We thank CNR (Progetto Finalizzato "Chimica Fine II" and Progetto Strategico "Tecnologie Chimiche Innovative"), Ministero per l'Universitá e la Ricerca Scientifica e Tecnologica (MURST 40%), and CNRS for financial support, and PUMEX S.p.A. for supplying pumice samples. L. F. L. thanks CNR for a leave of absence enabling a stay at the Institut de Recherches sur la Catalyse.

REFERENCES

1. Döbereiner, W., *Pogg. Ann.* **64**, 94 (1845).
2. Anderson, R. B., *in* "Catalysis" (P. H. Emmett, Ed.), Vol. IV, pp. 123 and 332. Reinhold, New York, 1956.
3. Mross, W. D., *Catal. Rev. Sci. Eng.* **25**, 591 (1983).
4. Van der Lee, G., Bastein, A. G. T., van der Borgert, J., Schuller, B., Luo, H., and Ponec, V., *J. Chem. Soc., Faraday Trans. I* **83**, 2103 (1987).
5. Praliaud, H., Dalmon, J. A., Martin, G. A., Primet, M., and Imelik, B., C.R. Paris C291, 89 (1980).
6. Praliaud, H., Dalmon, J. A., Mirodatos, C., and Martin, G. A., *J. Catal.* **97**, 344 (1986).
7. Poutsma, M. L., Elek, L. F., Ibarbia, P. A., Risch, A. P., and Rabo, J. A., *J. Catal.* **52**, 157 (1978).
8. Kikuzono, Y., Kagami, S., Naito, S., Onishi, T., and Tamaru, K., *Chem. Lett. Chem. Soc. Japan* 1249 (1981).
9. Kikuzono, Y., Kagami, S., Naito, S., Onishi, T., and Tamaru, K., *Faraday Discuss. Chem. Soc.* **72**, 135 (1981).
10. Kagami, S., Naito, S., Kikuzono, Y., and Tamaru, K., *J. Chem. Soc. Chem. Comm.* 256 (1983).
11. Yoshioka, H., Naito, S., and Tamaru, K., *Chem. Lett. Chem. Soc. Japan* 981 (1983).
12. Orita, H., Naito, S., and Tamaru, K., *Chem. Lett. Chem. Soc. Japan* 1161 (1983).
13. Rieck, J. S., and Bell, A. T., *J. Catal.* **100**, 305 (1986).
14. Park, Y. H., and Price, G. L., *J. Chem. Soc. Chem. Comm.* 1188 (1991).

15. Pitchon, V., Guenin, M., and Praliaud, H., *Appl. Catal.* **63**, 333 (1990).
16. Venezia, A. M., Duca, D., Floriano, M. A., Deganello, G., and Rossi, A., *SIA Surf. Interface Anal.* **18**, 619 (1992).
17. Venezia, A. M., Duca, D., Floriano, M. A., Deganello, G., and Rossi, A., *SIA Surf. Interface Anal.* **19**, 543 (1992).
18. Venezia, A. M., Rossi, A., Duca, D., Martorana, A., and Deganello, G., *Appl. Catal. A* **125**, 113 (1995).
19. Deganello, G., Duca, D., Liotta, L. F., Martorana, A., and Venezia, A. M., *Gazz. Chim. It.* **124**, 229 (1994).
20. Deganello, G., Duca, D., Martorana, A., Fagherazzi, G., and Benedetti, A., *J. Catal.* **150**, 127 (1994).
21. Duca, D., Liotta, L. F., and Deganello, G., *J. Catal.* **154**, 69 (1995).
22. Duca, D., Liotta, L. F., and Deganello, G., *Catal. Today* **24**, 15 (1995).
23. Duca, D., Frusteri, F., Parmaliana, A., and Deganello, G., *Appl. Catal. A*, in press.
24. Che, M., and Bennett, C. O., *Adv. Catal.* **36**, 55 (1989).
25. Bond, G. C., *Chem. Soc. Rev.* **20**, 441 (1991).
26. Boitiaux, J. P., Cosyns, J., and Vasudevan, S., *in* "Preparation of Catalysts III" (G. Poncelet, P. Grange, and P. A. Jacobs, Eds.), p. 123. Elsevier, Amsterdam, 1983.
27. Boitiaux, J. P., Cosyns, J., and Vasudevan, S., *Appl. Catal.* **6**, 4 (1983).
28. Takasu, Y., Unwin, R., Tesche, B., Bradshaw, A. M., and Grunze, M., *Surf. Sci.* **77**, 219 (1978).
29. Mason, M. G., *Phys. Rev. B* **27**, 748 (1983).
30. Pitchon, V., Gallezot, P., Nicot, C., and Praliaud, H., *Appl. Catal.* **47**, 357 (1989).
31. Liotta, L. F., Deganello, G., Delichère, P., Leclercq, C., and Martin, G. A., *J. Catal.* **164** (1996).
32. Pitchon, V., Primet, M., and Praliaud, H., *Appl. Catal.* **62**, 317 (1990).
33. Liotta, L. F., Venezia, A. M., Martorana, A., Duca, D., and Deganello, G., to be submitted.
34. Wisseberger, A., and Proskauer, E.S., *in* "Organic Solvents" Vol. VII. Interscience, New York, 1955.
35. Vicarini, M. A., Nicolaon, G. A., and Teichner, S. J., *Bull. Soc. Chim. Fr.* 1466 (1969), and references therein.
36. Carturan, G., Gottardi, G., and Graziani, M., *J. Non-Cryst. Solids* **29**, 41 (1978).
37. Carturan, G., and Strukul, G., *J. Catal.* **57**, 516 (1979).
38. Gubitosa, G., Serton, A., Camia, M., and Pernicone, N., *in* "Preparation of Catalysts III" (G. Poncelet, P. Grange, and P. A. Jacobs, Eds.), p. 431. Elsevier, Amsterdam, 1983.
39. Benesi, H. A., Curtis, R. M., and Studer, H. P., *J. Catal.* **10**, 328 (1968).
40. Fuentes, S., and Figueras, F., *J. Chem. Soc. Farad. Trans.* **74**, 174 (1978).
41. Aben, P. C., *J. Catal.* **10**, 224 (1968).
42. Benson, J. E., Wang, H. S., and Boudart, M., *J. Catal.* **39**, 146 (1973).
43. Fagherazzi, G., Benedetti, A., Deganello, G., Duca, D., Martorana, A., and Spoto, G., *J. Catal.* **150**, 117 (1994).
44. Eischens, R. P., Francis, S. A., and Pliskin, W. A., *J. Phys. Chem.* **60**, 194 (1956).
45. Eischens, R. P., and Pliskin, W. A., *Adv. Catal.* **10**, 1 (1958).
46. Naccache, C., Primet, M., and Mathieu, M. V., *Adv. Chem. Ser.* **121**, 266 (1973).
47. Figueras, F., Gomez, R., and Primet, M., *Adv. Chem. Ser.* **121**, 460 (1973).
48. Vannice, M. A., Wang, S. Y., and Moon, S. H., *J. Catal.* **71**, 152 (1981).
49. Hicks, R. F., Yen, Q. J., and Bell, A. T., *J. Catal.* **89**, 498 (1981).
50. Vannice, M. A., and Wang, S. Y., *J. Phys. Chem.* **85**, 2543 (1981).
51. Gelin, P., Siedle, A. R., and Yates, J. T., *J. Phys. Chem.* **88**, 2978 (1984).
52. Sheu, L. L., Karpinski, Z., and Sachtler, W. M. H., *J. Phys. Chem.* **93**, 4890 (1989).
53. Bradshaw, A. M., and Hoffmann, F. M., *Surf. Sci.* **72**, 513 (1978).
54. Ortega, A., Hoffmann, F. M., and Bradshaw, A. M., *Surf. Sci.* **119**, 79 (1982).
55. Hoffmann, F. M., *Surf. Sci. Report* **3**, 107 (1983).
56. Greenler, R., Burch, K., Kretschmar, K., Klanser, R., Bradshaw, A. M., and Hayden, B., *Surf. Sci.* **338**, 152 (1985).
57. Brum Pereira, E., and Martin, G. A., *Appl. Catal. A* **103**, 291 (1993).
58. Palazov, A., Chang, C. C., and Kokes, R. J., *J. Catal.* **36**, 338 (1975).
59. Martin, G. A., and Praliaud, H., *Catal. Lett.* **9**, 151 (1991).
60. Horwitz, C. P., and Shriver, D. F., *Adv. Organometal Chem.* **23**, 219 (1984).
61. Uram, K. J., Ng, L., Folman, M., and Yates, J. T., *J. Chem. Phys.* **84**, 2891 (1986).
62. Holloway, S., Nørskov, J. K., and Lang, N. D., *J. Chem. Soc. Faraday Trans. I* **83**, 1935 (1987).
63. MacLaren, J. M., Vvedensky, D. D., Pendry, J. B., and Joyner, R. W., *J. Chem. Soc. Faraday Trans. I* **83**, 1945 (1987).
64. Dose, V., Rogozik, J., Bradshaw, A. M., and Prince, K. C., *Surf. Sci.* **179**, 90 (1987).
65. Praliaud, H., Primet, M., and Martin, G. A., *Appl. Surf. Sci.* **17**, 107 (1983).
66. Praliaud, H., Primet, M., and Martin, G. A., *Bull. Soc. Chim.* **5**, 719 (1986).
67. Praliaud, H., Tardy, B., Bertolini, J. C., and Martin, G. A., *in* "Structure and Reactivity of Surfaces" (C. Morterra, A. Zecchina, and G. Costa, Eds.), p. 749. Elsevier, Amsterdam, 1989.
68. Angevaare, P. A. J. M., Hendrickx, H. A. C. M., and Ponec, V., *J. Catal.* **110**, 11 (1988).
69. Angevaare, P. A. J. M., Hendrickx, H. A. C. M., and Ponec, V., *J. Catal.* **110**, 18 (1988).
70. Berkó, A., and Solymosi, F., *J. Chem. Phys.* **90**, 2492 (1989).
71. Joyner, R. W., and Roberts, M. W., *J. Chem. Soc. Faraday Trans. I* **70**, 1819 (1974).
72. Eastman, D. E., Demuth, J. E., and Baker, H. M., *J. Vac. Sci. Technol.* **11**, 273 (1974).
73. Barber, M., Vickerman, J. C., and Wolstenholme, J., *J. Chem. Soc. Faraday Trans. I* **72**, 40 (1976).
74. Martin, G. A., Primet, M., and Dalmon, J. A., *J. Catal.* **53**, 321 (1978).
75. Ueno, A., and Bennett, C. O., *J. Catal.* **54**, 31 (1978).
76. Solymosi, F., and Knözinger, H., *J. Catal.* **122**, 166 (1990).
77. Raskó, J., and Solymosi, F., *J. Phys. Chem.* **98**, 7147 (1994).
78. Venezia, A. M., Rossi, A., Liotta, L. F., Martorana, A., and Deganello, G., *Appl. Catal. A*, in press.
79. Chesters, M. A., Mc Douglas, G., Pemble, M., and Sheppard, N., *Surf. Sci.* **16**, 425 (1985).
80. Rieck, J. S., and Bell, A. T., *J. Catal.* **100**, 305 (1986).
81. Hoffmann, F. M., and Bradshaw, A. M., *J. Catal.* **44**, 328 (1976).
82. Liotta, L. F., unpublished data (1995).
83. Pitchon, V., Praliaud, H., and Martin, G. A., *in* "Natural Gas Conversion" (A. Holmen *et al*., Eds.), p. 265. Elsevier, Amsterdam, 1991.